

## AN ANALYSIS OF CYLINDRICAL BORIS SOLVER FOR TYPICAL PARAMETERS OF TWO-DIMENSIONAL PENNING ION SOURCE SIMULATION

### ANALISIS PEMECAH BORIS SILINDER UNTUK PARAMETER TIPIKAL DARI SIMULASI SUMBER ION PENNING DUA DIMENSI

Ahsani Hafizhu Shali<sup>1,\*</sup>, Ahmad Hasan As'ari<sup>2</sup>

<sup>1</sup>Research Center for Accelerator Technology, National Research and Innovation Agency (BRIN), Kawasan Sains dan Teknologi B.J. Habibie, Tangerang Selatan, 15340

<sup>2</sup>Research Center for Advanced Materials, National Research and Innovation Agency (BRIN), Kawasan Sains dan Teknologi B.J. Habibie, Tangerang Selatan, 15314

\*Corresponding author e-mail: [ahsani.hafizhu@batan.go.id](mailto:ahsani.hafizhu@batan.go.id)

Received 19 January 2023, revised 17 July 2023, accepted 30 July 2023

#### ABSTRACT

**AN ANALYSIS OF CYLINDRICAL BORIS SOLVER FOR TYPICAL PARAMETERS OF TWO-DIMENSIONAL PENNING ION SOURCE SIMULATION.** The cylindrical Boris solver is analyzed for typical two-dimensional Penning ion source simulation parameters. The analysis comprises the solver's accuracy and stability, especially for the latter simulation stages, typically after about 30  $\mu$ s. The simulation is done for two cases; the first is a gyration simulation with a homogenous magnetic field, and the second uses the same setup as the Penning simulation. Several investigated quantities to determine the error are the radial position, axial position, and velocity magnitude (or kinetic energy). The error is calculated by comparing the result with the reference result from the exact solver with an incredibly small time step width,  $dt = 10^{-15}$  s. The result shows a discrepancy between cylindrical and cartesian Boris solvers. The velocity magnitude of the particle decays as time goes on for the cylindrical Boris solver, especially when the particle is close to the z-axis, an error not found on the cartesian solver. For typical Penning simulation parameters, the trajectory of individual particles is way off the reference trajectory. However, the mean position is relatively close to the reference compared to the dimension of the simulation domain. The kinetic energy is also relatively accurate, with a similar slow decay related to the deteriorating non-axial velocity components previously observed in the first case. Thus, for the simultaneous simulation of millions of particles, there should not be any significant observable difference in actual Penning simulation compared to Penning simulation with reference time step width.

**Keywords:** Cylindrical Boris solver, Penning ion source, simulation

#### ABSTRAK

**ANALISIS SOLVER BORIS SILINDRIS UNTUK PARAMETER TIPIKAL SIMULASI SUMBER ION PENNING DUA DIMENSI.** Pemecah Boris silindris dianalisis untuk parameter tipikal simulasi sumber ion Penning dua dimensi. Analisis terdiri dari akurasi dan stabilitas pemecah, terutama untuk tahap akhir simulasi, yang biasanya setelah sekitar 30  $\mu$ s. Simulasi dilakukan untuk dua kasus, yang pertama adalah simulasi girasi dengan medan magnet homogen, sedangkan kasus kedua menggunakan pengaturan yang sama persis dengan simulasi Penning. Beberapa besaran yang diselidiki untuk menentukan kesalahan adalah posisi radial, posisi aksial, dan besaran kecepatan (atau energi kinetik). Kesalahan dihitung dengan membandingkan hasil dengan hasil referensi dari pemecah yang sama dengan lebar langkah waktu yang sangat kecil,  $dt=10^{-15}$  s. Hasilnya menunjukkan bahwa ada perbedaan antara pemecah Boris silinder dan kartesius. Besaran kecepatan partikel meluruh seiring berjalannya waktu untuk pemecah Boris berbentuk silinder terutama ketika partikel mendekati sumbu z, kesalahan tidak ditemukan pada pemecah kartesius. Untuk parameter simulasi Penning tipikal, lintasan partikel individu jauh dari lintasan referensi. Namun, posisi rata-rata relatif dekat dengan referensi dibandingkan dengan dimensi domain simulasi. Energi kinetik juga relatif akurat, dengan peluruhan lambat serupa terkait dengan komponen kecepatan non-aksial yang memburuk yang sebelumnya diamati pada kasus pertama. Dengan demikian, untuk simulasi jutaan partikel secara simultan, seharusnya tidak ada perbedaan signifikan yang dapat diamati pada simulasi Penning aktual dibandingkan dengan simulasi Penning dengan lebar langkah waktu referensi.

**Kata kunci:** Boris silinder, Penning, sumber ion, simulasi

## INTRODUCTION

**B**oris algorithm is currently the most popular method for numerically solving the equation of motion of magnetized plasma [1]. Its simplicity and accuracy have it relevant for more than fifty years in the field of computational plasma [2]. Simplicity is necessary for plasma simulation with kinetic methods (such as the particle-in-cell method), where millions of macroparticles are simulated simultaneously inside the domain. A more objective approach can also be utilized, but higher computational power is needed (possibly longer simulation time too). So far, the Boris algorithm is at the sweet spot between accuracy and simplicity [3].

Several advances in numerical simulation of plasma (and computers are much more potent than decades ago) made it possible for complex simulation. Some simulations, such as plasma interaction with high-frequency electromagnetic fields, generally require many simulation steps [4], while in general, all particle integrators (such as the Boris algorithm) will accumulate errors over time. Thus, it is crucial to ensure that such a simulation's accuracy is retained in later periods.

The Center for Accelerator Technology Research (PRTA) is developing a magnetized plasma simulation code to optimize the Penning ion source. The ion source produces  $H^+$  in the DECY-13 cyclotron built in PRTA [5]. The penning ion source has a cylinder shape where the bases are given a fixed (negative) electric potential while the side is grounded, as seen in Figure 1 [6]. An axial magnetic field is applied to the ion chamber, which causes electrons to oscillate, making ionization more efficient [7].

The result published by [8] shows that Penning discharge simulation requires a million iterations to get a stationary result. It is then essential to make sure that the particle integrator stays accurate at a later time. Additionally, since the domain for Penning discharge simulation is cylindrical, it is generally more desired to do a simulation in two spatial dimensions (in  $r$ - $z$  coordinate). Three-dimensional simulation is possible, but the number of nodes will increase at least ten-fold, slows the simulation considerably.

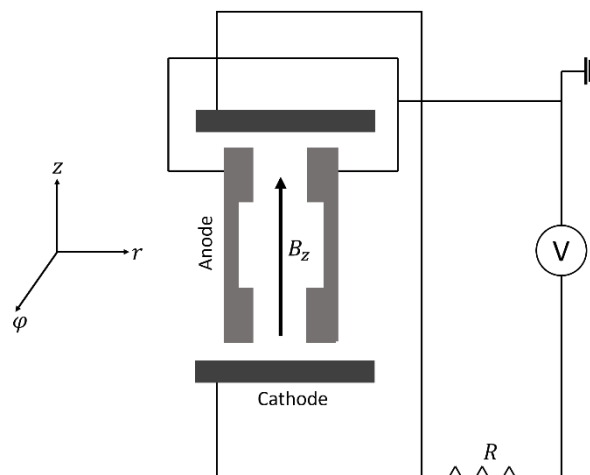


**Figure 1.** The schematics of the Penning ion source

The equation of motion in cylindrical coordinates differs from that in cartesian coordinates because of inertial force terms [9]. For Penning discharge simulation, however, it is not recommended to solve the cylindrical equation of motion as it is since there will be particles close to the  $z$ -axis (thus  $r = 0$ ), which will likely produce numerical error from the inertial terms. Boris proposed circumventing this problem by calculating the position part in cartesian coordinates while the velocity part is calculated in cylindrical coordinates without inertial forces terms. The inertial forces are mimicked by rotating the reference frame of each particle, such that in the new frame, the  $y$ -position of the particle is equal to zero. The velocity needs to be rotated back following the rotation of position. A detailed analysis of this topic can be found in [10]. Unfortunately, to date, no published paper thoroughly analyzes the accuracy of Boris solver in the region of a type parameter value of Penning discharge simulation.

This paper investigates the accuracy and stability of a two-dimensional cylindrical Boris solver for typical Penning discharge simulation parameters. Velocity back rotation may incur additional errors previously not found without that scheme.

Boris algorithm is first derived by discretizing the Lorentz equation for charged particles in a leap-frog-like manner given below [11,12]

$$\vec{x}^{n+1} = \vec{x}^n + \vec{v}^{n+0.5} \Delta t \quad (1)$$

$$\vec{v}^{n+0.5} = \vec{v}^{n-0.5} + \frac{q\Delta t}{m} [\vec{E}(\vec{x}^n) + \vec{v} \times \vec{B}(\vec{x}^n)] \quad (2)$$

Note that the expressions above are written in cartesian coordinates. Similar equations for cylindrical coordinates require additional inertial force terms on the velocity update. For Boris algorithm, the averaged velocity  $\vec{v}$  is defined by

$$\vec{v} = \frac{\vec{v}^{n+0.5} + \vec{v}^{n-0.5}}{2} \quad (3)$$

To get  $\vec{v}^{n+0.5}$  given  $\vec{v}^{n-0.5}$ ,  $\vec{v}$  from equation (3) is then substituted into equation (2). At first, it seems that the result will be implicit since there is  $\vec{v}^{n+0.5}$  crossed with magnetic induction  $\vec{B}$  at the right-hand side of equation (2). However, it can be solved explicitly by separating the equation's electric field and magnetic field contribution. So, two new variables are defined as follows:

$$\vec{v}^{n-0.5} = \vec{v}^- - \frac{q\Delta t \vec{E}(\vec{x}^n)}{2m} \quad (4)$$

$$\vec{v}^{n+0.5} = \vec{v}^+ + \frac{q\Delta t \vec{E}(\vec{x}^n)}{2m} \quad (5)$$

The following equation is obtained by substituting both of them to equation (2).

$$\vec{v}^+ - \vec{v}^- = \frac{q\Delta t}{m} \left[ \frac{\vec{v}^+ + \vec{v}^-}{2} \right] \times \vec{B}(\vec{x}^n) \quad (6)$$

Since the contribution of the electric field has been taken out, the magnitude of  $\vec{v}^+$  and  $\vec{v}^-$  is equal. Hence the process is purely rotational.  $\vec{v}^+ - \vec{v}^-$  can be calculated using geometrical interpretation. The standard two-step procedure is given below (it is possible to use several steps to get a more accurate result, see [13])

$$\vec{v}' = \vec{v}^- + \vec{v}^- \times \vec{t} \quad (7)$$

$$\vec{v}^+ = \vec{v}^- + \vec{v}' \times \vec{s} \quad (8)$$

where  $\vec{t} = \frac{q\Delta t \vec{B}(\vec{x}^n)}{2m}$  and  $\vec{s} = \frac{2\vec{t}}{1+t^2}$ . Thus, for cartesian coordinates, at least, it is possible to get  $\vec{x}^n$  and  $\vec{v}^{n+0.5}$  at every time step gave an initial condition. For a cylindrical coordinate, however, equation (2) requires an additional term that is  $\vec{F}_{in}$  or inertial force. The components of equation (2) can be written as follows

$$\frac{dv_r}{dt} = \frac{q}{m} (E_r + v_\theta B_z - v_z B_\theta) + \frac{v_\theta^2}{r} \quad (9)$$

$$\frac{dv_\theta}{dt} = \frac{q}{m} (E_\theta + v_z B_r - v_r B_z) - \frac{v_r v_\theta}{r} \quad (10)$$

$$\frac{dv_z}{dt} = \frac{q}{m} (E_z + v_r B_\theta - v_\theta B_r) \quad (11)$$

The two last terms in equations (9) and (10) are the components of inertial force on cylindrical coordinates. As can be seen, there will be singularity for  $r = 0$  when either  $v_r$  or  $v_\theta$  are non-zero. Boris suggested circumventing this by calculating the position part in cartesian coordinates, while the velocity part is calculated in cylindrical coordinates but without inertial force terms. The inertial forces are mimicked by rotating the cartesian coordinate in position update so that the new x-component in the new coordinate equals the particle's distance to the origin in the previous coordinate (the y-component in the new coordinate is always equal to zero). Since the particle is in a new coordinate, the velocity must be rotated accordingly. The illustration can be seen in Figure 2, shown below.

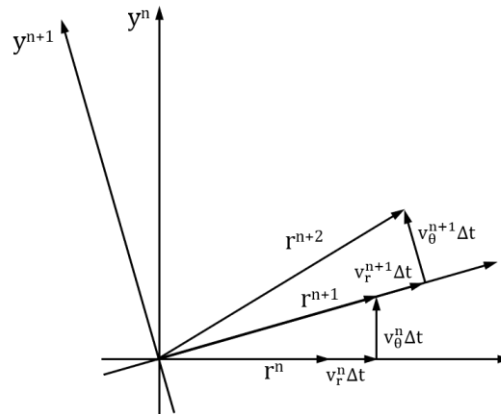


Figure 2. Coordinate transformation for cylindrical Boris algorithm [10]

The steps to coordinate rotation are given as follows. The distance between the particle and the origin and the angle of rotation after particle push is calculated as follows

$$r = \sqrt{x'^2 + y'^2} \quad (12)$$

$$\alpha = \arctan\left(\frac{y'}{x'}\right) \quad (13)$$

And thus, after rotation, the position of the particle in cartesian coordinates is given by  $\vec{x} = (r, \mathbf{0}, z)$ . The velocity is also rotated by  $\alpha$  along the z-axis as the following

$$v_r' = \cos \alpha v_r + \sin \alpha v_\theta \quad (14)$$

$$v_\theta' = -\sin \alpha v_r + \cos \alpha v_\theta \quad (15)$$

By using that method, errors because of singularity in equations (9) and (10) can be avoided. This is important when the cylindrical coordinate is the only option to do simulation, especially when  $r = \mathbf{0}$  is included in the domain, such as in two-dimensional Penning discharge (z-r coordinate). Delzanno has also emphasized the importance of choosing the correct initial condition for the Boris solver in cylindrical coordinates, as choosing the wrong initial condition might reduce the overall accuracy of the cylindrical Boris solver.

Several authors have pointed out the strengths of the Boris algorithm, such as having second-order accuracy while only requiring single-step evaluation and that it conserves energy precisely in the absence of an electric field [1,3]. Nevertheless, as can be seen from equation (12) to equation (15), several modifications to the original algorithm (in cartesian coordinate) were added. This modification might affect the overall accuracy of the algorithm, especially for a large number of steps. The algorithm's accuracy can be analyzed by comparing the result obtained with the standard three-dimensional method in the cartesian coordinate.

## METHODOLOGY

Two cases for the cylindrical Boris algorithm are then investigated:

- A case with homogenous and static magnetic fields and zero electric fields (gyration test).
- A case where the magnetic field is static and homogenous, but the electric field follows the typical distribution of the Penning ion source.

The simulation uses an electron as a test particle since it is the most ubiquitous particle type in Penning simulation.

The initial velocity is chosen for electrons around the energy of interest in the Penning discharge process, specifically for kinetic energy  $T = 1.3$  and  $30$  eV. That kinetic energy is relevant for the dissociative attachment process [14], for the typical initial kinetic energy of penning discharge [15], and for the ionization process of Hydrogen atoms [16]. Abadi chose  $30$  ps for the time step width on his Penning discharge simulation. It is thus interesting to see if it is possible to use a higher time step width since doing so would reduce the computational resource needed to run the simulation. However, the time step width must not be larger than the gyration period of the particle, which is a function of the magnetic field, which is given by  $T = 2\pi m/qB$ . Thus, the larger the magnetic field is, the smaller the maximum possible time step width must be.

The time step value is relevant to the predicted time needed for the equilibrium to occur in the Penning discharge simulation (which is equal to time step width  $\times$  time steps). Abadi et al. show that for time step width  $dt = 30$  ps, the plasma is in equilibrium after one million iterations or about  $30 \mu s$ .

For the second case, the following simplified model of the Penning ion source is used.

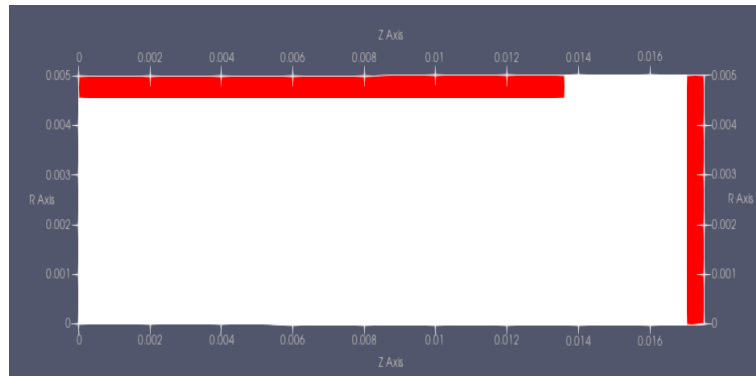


**Figure 3.** Simplified model of the domain of Penning simulation

As mentioned previously, the domain is simplified into a two-dimensional r-z plane based on the azimuthal symmetry of the system. The red area in Figure 3 represents a copper sheath (which means that the simulated particle cannot go there), while the white area represents a vacuum. At  $z = 0.017$  m, the cathode is given a fixed potential  $V = -700$  volt, while the sheath at  $r = 0.005$  m is electrically grounded. The mirror symmetry of the Penning ion source concerning the plane perpendicular to the z-axis can further simplify the problem. Because of symmetry, any particle crossing the  $z = 0$  plane has reflected the domain, with its axial velocity reversed.

The error for each case (compared to the reference) is calculated using the following scheme, similar to Delzanno [10]. The equations are given by:

$$\text{Err}_i = \sqrt{\frac{\sum_j |q_{iref}^j - q_i^j|^2}{N}} \quad (16)$$

$q_i^j$  is the i-th parameter (such as radial position, radial velocity, axial position, etc.) at the j-th step, and N is the total of the steps. The time step width for case 1 and case 2 is the same, which is  $dt_{ref} = 10^{-15}$  s. It is 30000 times smaller than the typically used time step width  $dt = 3 \times 10^{-11}$  s.

Given a set of parameters, the error for both cases is examined for several values of time step width. The variation of time step width might be significant, especially for case 2, where the electric field distribution is not that simple, which might cause the accumulation of errors to give a different particle trajectory. The chosen time step widths for both cases are shown in Table 1.

**Table 1.** Time step width used for simulation

No	Divisor	Time step width (s)
1	1	$3 \times 10^{-11}$
2	2	$1.5 \times 10^{-11}$
3	3	$1 \times 10^{-11}$
4	4	$7.5 \times 10^{-12}$
5	5	$6 \times 10^{-12}$
6	6	$5 \times 10^{-12}$
7	8	$3.75 \times 10^{-12}$
8	10	$3 \times 10^{-12}$
9	15	$2 \times 10^{-12}$
10	20	$1.5 \times 10^{-12}$
11	25	$1.2 \times 10^{-12}$
12	30	$1 \times 10^{-12}$
13	50	$6 \times 10^{-13}$
14	100	$3 \times 10^{-13}$
15	200	$1.5 \times 10^{-13}$

Since the errors from different time steps (because the time step widths are different) are compared, it is only fair to choose a set of fixed time steps related to the case with the most prominent step width. Only data from the same time steps ( $t^n$ ) that is going to be compared, where ( $t^n$ ) are time steps for  $dt = 30$  ps.

The specific method used to measure the error for case 1 and case 2 is described below.

1. Case 1

The objective of the first case is to calculate the accuracy and stability of the cylindrical Boris solver for typical parameters of Penning simulation. The point of the cylindrical Boris solver is to avoid singularity from inertial forces, as explained in the previous section [11]. Nevertheless, it is also evident from Taylor's expansion that the accuracy of the cylindrical Boris algorithm is proportional to  $1/r$  [10]. It is possible that even if the singularity is not present, the algorithm becomes wildly inaccurate.

Delzanno et al. have derived the accuracy of the cylindrical Boris algorithm in the absence of a magnetic field [10]. In the presence of a magnetic field, the accuracy is rather difficult to calculate because of the coupling of various components of the equation of motion from the Lorentz force. However, since the inertial forces are still present, the accuracy is expected to depend on  $1/r$ . Thus in case 1, the accuracy of the cylindrical Boris solver with the presence of an axial magnetic field (without an electric field) for various initial radii is typically used in Penning simulation.

The reference case for case 1 is calculated using the Boris-A solver in the cartesian coordinate [2]. The cartesian Boris solver is chosen since the inertial force problem is non-existent, while the type-A solver gives a more accurate gyration part (which translates to a more accurate position in cylindrical coordinates). The result from the cartesian coordinate is thus transformed into a cylindrical coordinate using the following transformation

$$r = \sqrt{x^2 + y^2} \tag{17}$$

$$\theta = \tan^{-1} \left( \frac{y}{x} \right) \tag{18}$$

$$v_r = \cos \theta v_x + \sin \theta v_y \tag{19}$$

$$v_\theta = -\sin \theta v_x + \cos \theta v_y \tag{20}$$

Figure 4 shows the expected trajectory of case 1 test, where electric field is non-existent, and the initial velocity of the particle is perpendicular to the direction of magnetic field. The gyration angle (indicated by angle  $\alpha$  in Figure 4) is generally unimportant in simulations using a cylindrical Boris solver [16]. Thus, the accuracy of the gyration angle is not investigated here. Two interesting parameters that will be compared are the radial position of the particle (from the z-axis) and the magnitude of the velocity. For a system with a non-zero magnetic field and zero electric fields, the velocity magnitude indicates the kinetic energy and the radius of gyration. The accuracy of kinetic energy is vital for simulations that employ the Monte-Carlo collision algorithm to simulate short-range interaction between particles [18], such as in the Penning ion source simulation [19].

Velocity components are rather complicated to calculate because of the rotating coordinate in the cylindrical Boris solver. Assuming some errors on the gyration angle, the coordinate axis chosen for specific steps would be different for different values of time step width. Thus, comparing velocity components of two different time step widths is impossible unless some fixed coordinate axis is used.

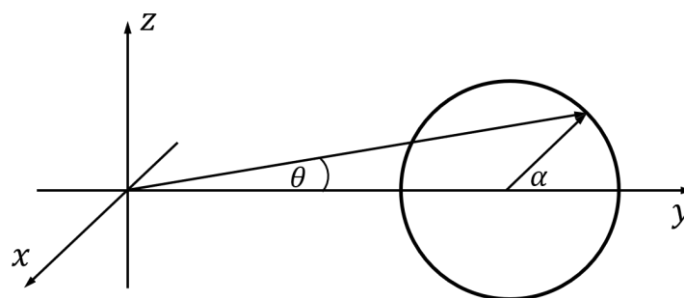


Figure 4. Expected particle trajectory for case 1 ignoring possible numerical errors

The error for case 1 is calculated using equation (16). The reference data is calculated using the more accurate Boris-A algorithm in cartesian coordinates and then transformed into a cylindrical coordinate. Boris-A algorithm has a better gyration accuracy than the standard Boris algorithm, which is ideal for reference in this case. The difference between them lies in the definition of  $\vec{t}$  from equation (7), wherein Boris-A case,  $\vec{t} = \tan \left( \frac{q\Delta t \vec{B}(\vec{x}^n)}{2m} \right)$ .

The value of parameters used in this simulation is summarized in Table 2, where the initial radial position is related to the dimension of a typical Penning ion source chamber.

**Table 2.** Simulation parameters for case 1

Magnetic Field Strength (T)	Initial kinetic energy (eV)	Initial radial position (mm)
0.1	1	0.1
0.7	3	1
1.25	30	3

## 2. Case 2

Axisymmetrical domain is used in case 2, with mirror symmetry at  $z = 0$  plane. The domain follows the setup from the Penning simulation paper by Abadi, with the exact meshing. The radius of the cylinder is 5 mm, while the height is 17 mm. The domain has meshed into a  $35 \times 10$  rectangular cell (rectangular in  $r$ - $z$  coordinate). The electric potential distribution from the boundary condition is seen in Figure 3.



**Figure 5.** Electric potential distribution inside the ion chamber

As seen in Figure 1, the cathode is placed on the cylinder's top (and bottom) while the sheath is grounded. The value of electric potential on the cathode and anode is used as the boundary condition for the potential solver. As seen from Figure 3,  $z = 0$  and  $r = 0$  lines are open boundaries resulting from domain symmetry. The electric potential on each node (other than on the cathode and anode) is calculated using the Gauss-Seidel method [16]. A small tolerance value can be used here since the potential is only calculated once at the beginning of the simulation. Here, the tolerance is set to 0.001 volts. The electric field on each node is calculated using the finite difference method, using the second-order forward (backward) difference for nodes in the leftmost and bottom boundaries (rightmost and upper boundaries). In contrast, the rest of the nodes are calculated using the first-order central difference method [16]. The value of the electric field at the position of the simulated particle is obtained using the first-order interpolation algorithm [17].

This simulation's magnetic field is homogenous and directed to the negative  $z$  direction. Because of that, there is no need to store the value of the magnetic field on discrete nodes. The assumption is based on the approximation of magnetic field distribution inside the Penning ion source developed in PRTA. One value of the axial magnetic field is used,  $B_z = 1.25$  T [20]. The value of the axial magnetic field is relevant to the Penning ion source used in PRTA.

The reference data for this case is calculated directly on a cylindrical coordinate since obtaining data from a cartesian coordinate means the simulation must run on three-dimensional domains. This generally will give a different result on potential calculation, especially if the chosen shape of the mesh is still hexahedral. Thus the reference data is calculated in cylindrical coordinates using the same time step width as case 1,  $dt = 10^{-15}$  s.

Several initial conditions are considered in this case. The initial position of the simulated particle is defined in several specific initial positions of particles on Penning simulation. Test cases have bigger time step width, just like case 1, since it is plausible to use in actual Penning simulation. The error is calculated using equation (16) for parameters such as position, velocity, and kinetic energy. It is possible for the simulated particle on the reference or test case to cross the boundary of the simulation. If the crossed boundary is the axis of symmetry, then the particle is reflected. Otherwise, the particle is deleted, and the simulation is stopped. Thus, the test case and the reference case can have different time steps. The maximum time step is decided by examining which case has its simulated particle outside the boundary.

The following figure shows the initial positions of the simulated particle:

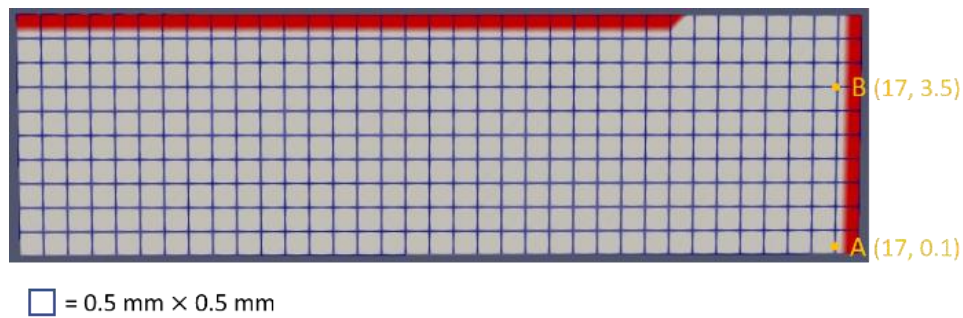


**Figure 6.** Two initial positions were used for case 2

Like case 1, the first initial position is chosen to be very small to see whether a small radial position will cause a significant error. However, the particle will not pick up a sizeable radial velocity for that position since the electric boundary conditions cause the electric field to point to the axial direction near the z-axis. Thus, for the first initial position, initial radial velocity related to the kinetic energy of 30 eV is also assumed. In Penning simulation, particles might have a large radial velocity resulting from scattering with other particles.

The long-term accuracy and stability of the cylindrical Boris equation for case 2 are also investigated. The particle's trajectory for several choices of divisor at the beginning of the simulation is compared to the trajectory of the particle at later times, where the measure of later times follows from the simulation by Abadi et al. [8]. To be more specific, the first 3 ns of the simulation is compared to the last 3 ns of the simulation, where the length of the simulation is 30  $\mu$ s.

## RESULT AND DISCUSSIONS

The first case to consider is where the electric potential equals zero. In this case, the particle's trajectory should be a perfect circle. The numerical error might slightly alter the shape of the trajectory. Nevertheless, an almost perfect circle is expected for the reference case, even for a vast time step. If the center of gyration is not located on the origin, then the radial position as a function of time will look like a sinusoidal function. Some results are presented below to get the first impression of the radial position as a function of time.

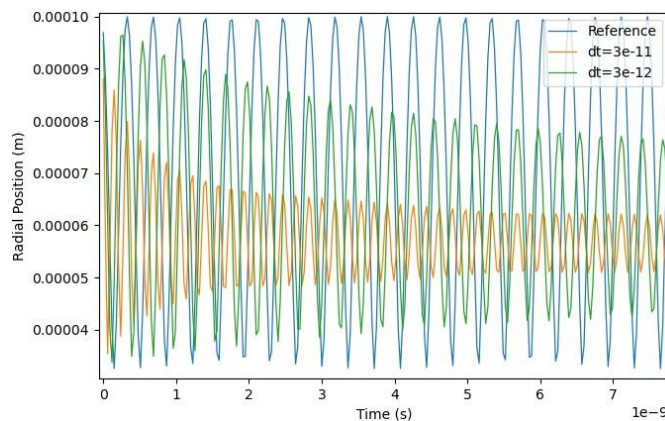


**Figure 7.** Radial position vs. time for  $B_z = 0.1$  T,  $E_k = 1$  eV,  $r_0 = 0.1$  mm

As seen from Figure 7 above, the radius of gyration of simulation with a more significant value of time step width  $dt$  will result in the faster decay of the radius of gyration. It is also evident from Figure 7 that there are bumps in the amplitude of the reference result, while it should have stayed constant. It is caused by the fact that data are sampled at a relatively rough time step, which is every 30 ps. A finer value of sample time steps will show that the amplitude is almost constant, which can be seen from the almost constant value of velocity amplitude of gyration.

Another critical thing to note is that the error of the gyration angle will cause the gyrating particle to have a different effective period of gyration. Because of that, it is difficult to compare the error of the radial position of the gyrating particle using equation 16. As an example, below is the calculated error for  $E_k = 1$  eV,  $r_0 = 0.1$  mm,

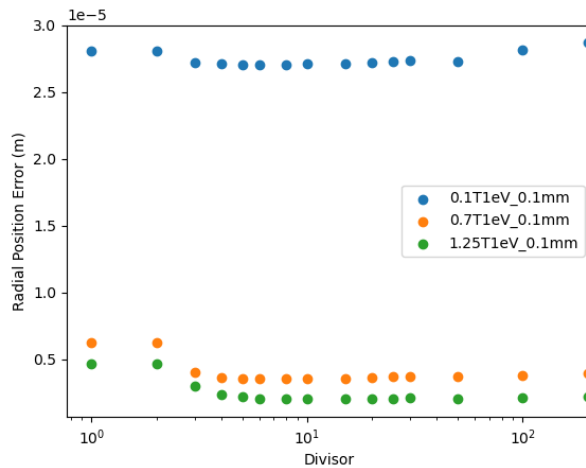


**Figure 8.** Radial position error (m) for several values of a divisor with  $E_k = 1$  eV and  $r_0 = 0.1$  mm

As can be seen from Figure 8, the calculated error of radial position is not consistent. Analytically, the bigger the divisor is, the smaller the error must be. As stated previously, this is because of gyration angle error, causing the simulation of different time step widths to be out of phase. From Figure 8, the decay is more prominent for bigger time step width, indicating that the error should have been more significant for larger time step width. It is possible to solve this discrepancy by calculating the error for a single period of gyration. Unfortunately, this is only possible when the time step width is smaller than the gyration period (at least twelve times smaller, so the gyration angle is 30 degrees for each step). The gyration period for an electron with  $B_z = 0.1, 0.7, 1.25$  tesla are  $T = 3.572 \times 10^{-10}, 5.103 \times 10^{-11}, 2.858 \times 10^{-11}$  second respectively. Thus, the smallest value of time step width from Table 1 is  $dt = 2$  ps. That assertion is also supported by the fact that the result for small divisors (where the time step width is larger than the period of gyration) does not make sense. The important point would be that the decay of the radius of gyration is proportional to the time step width. The quantitative error of the radius of gyration can be calculated using a magnitude of the velocity of the particle instead, which in this case is related by  $r = mv/qB$ .

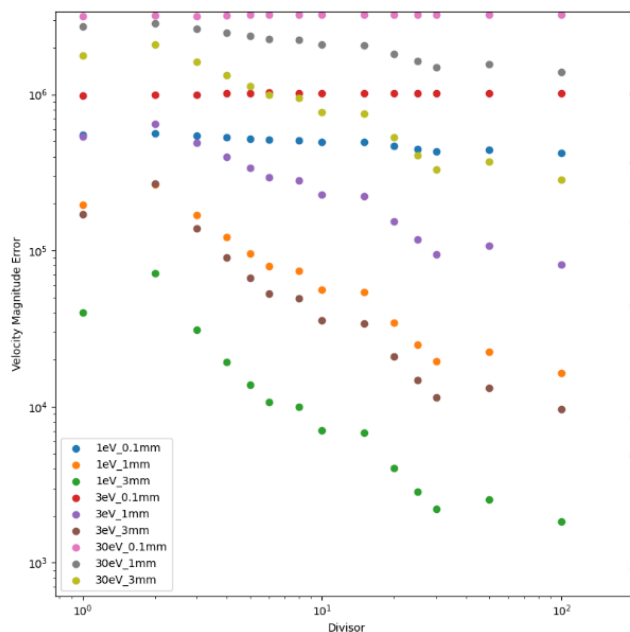


**Figure 9a.** Velocity magnitude error (m/s) vs. divisor for  $B_z = 0.1$  T

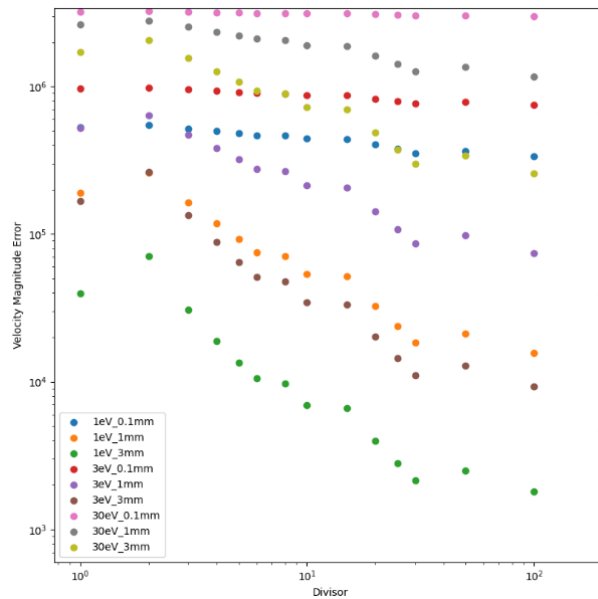


Figure 9b. Velocity magnitude error (m/s) vs. divisor for  $B_z = 0.7$  T

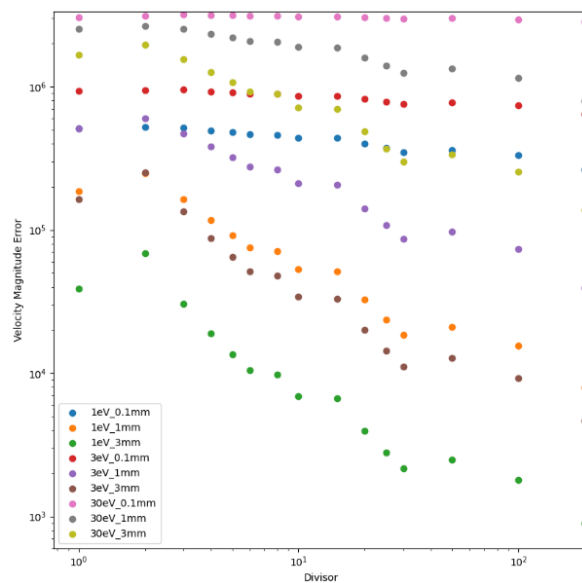
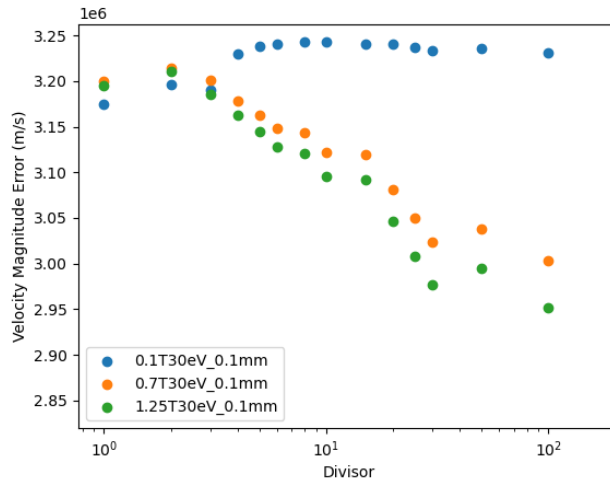


Figure 9c. Velocity magnitude error (m/s) vs. divisor for  $B_z = 1.25$  T

Several important points can be drawn from the results presented in Figure 9a-9c. The first one is that, generally, the error becomes larger the smaller the initial radial position of the particle is. For a wider choice of time step width, the minor initial position has an error of about ten times larger than the more prominent initial position. For small time step widths (such as when the divisor is 200), the error difference can be almost three orders of magnitude. The result shows that the closer the particle is, the larger the error becomes, even if the time step width is refined. At  $r = 0.1$  mm, the error does not drop significantly by reducing the time step width for all cases. The second point inferred from the three figures above is that higher initial energy will cause the error to be higher than the lower initial kinetic energy value. Two points mentioned above exhibit similar error properties of the cylindrical Boris solver shown by Delzanno [10], even though in his paper, the derivation is done with zero magnetic fields. Thus, this error is unique to the cylindrical Boris solver (with rotated reference axes). The initial objective of cylindrical Boris solver derivation was to avoid singularity when the simulated particle has a small, but it turns out that a small radial position will still give high error values.

The third important point is that axial magnetic field variation from  $B_z = 0.1$  T to  $B_z = 1.25$  T does not seem to give a significant difference in error. The comparisons of velocity magnitude error for different values of magnetic fields are presented below to give a clear impression of this matter. Two specific cases representing the highest error ( $r = 0.1$  mm  $E_k = 30$  eV) and the lowest error ( $r = 3$  mm,  $E_k = 1$  eV) are given as follows



**Figure 10.** Velocity magnitude error (m/s) vs. divisor for  $r = 0.1$  mm and  $E_k = 30$  eV

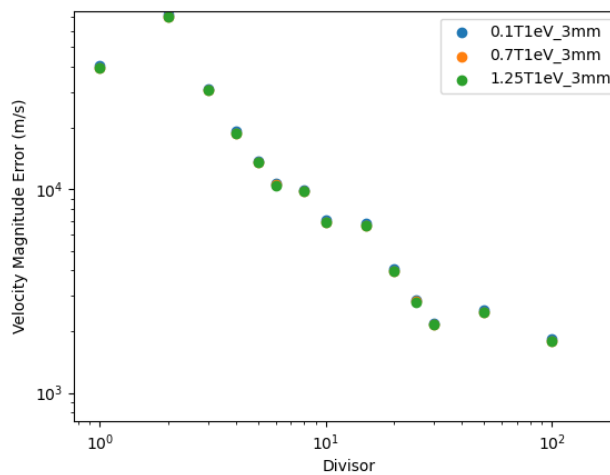


**Figure 11.** Velocity magnitude error (m/s) vs. divisor for  $r = 3$  mm and  $E_k = 1$  eV

For the high error case shown in Figure 10, it is clear that magnetic field strength influences the scheme's error. For considerable time step width (small divisor value), the error result does not make sense because of gyration error (the time step width is larger than the period of gyration, as mentioned previously). Figure 10 also shows that the radius of gyration affects the error calculation for the cylindrical Boris scheme. The radius of gyration for the case  $B_z = 0.1$  T is significantly larger than  $B_z = 0.7$  T. This might cause the origin to be located inside the gyration orbit, thus significantly increasing the error. It is not clearly understood why this is the case, but the sizeable radial position case ( $r = 3$  mm) indicates that the error is small when the gyration orbit of the particle is located far away from the origin. The case with  $B_z = 0.7$  T and  $B_z = 1.25$  T for  $r = 0.1$  mm and  $E_k = 30$  eV (small gyration radius) also shows that even if the error is significant, the error can be reduced by shrinking the time step width. The same thing cannot be said with  $B_z = 0.1$  T, supporting the hypothesis that the error will significantly increase when the origin is located inside the gyration orbit.

Figure 11 shows that the velocity magnitude error does not change by the appreciable amount for a relatively large initial particle radius. It indicates that a similar error value will be obtained for various magnetic field strengths as long as the particle is located relatively far from the origin.

The fourth point is that the velocity magnitude error does not always decrease with the decrease of time step width. Other than the case where the error increase when the time step width is shrunk from  $dt = 3 \times 10^{-11}$  to  $dt = 1.5 \times 10^{-11}$ , which is probably caused by gyration phase error, it can be seen that the error also increases when

the divisor is increased from 30 to 50. The plot for velocity magnitude with divisor = 25, 30, and 50 is presented below.

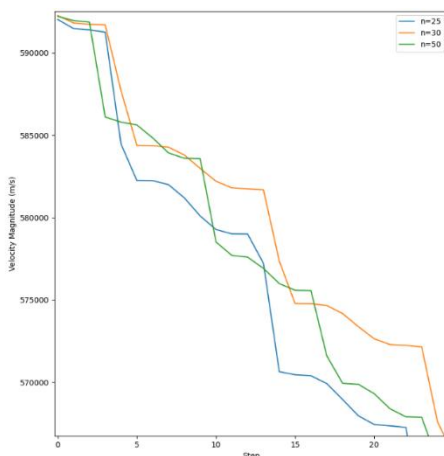


**Figure 12.** Velocity magnitude (m/s) vs. iteration step for several divisors

It is evident that initially, the velocity magnitude with a divisor of  $n = 50$  is the most accurate. However, the velocity dropped earlier than a divisor of  $n = 25$ . The velocity magnitude for  $n=50$  dropped the least compared to the other ones, but it dropped the most often, causing the case with  $n=30$  to have the least amount of velocity decay. It appears that the decay of velocity happened in a serialized fashion. The velocity error has something to do with the particle's position, where the error is calculated, specifically by the gyration angle. The case with a bigger divisor has a minor error in gyration angle, but velocity updates involve rotation from equations (14) and (15), which might have a numerical error that depends on the ratio of  $x$  and  $y$ . For comparison, the reference case calculated in cartesian coordinate (without coordinate rotation) does not experience any velocity magnitude decay.

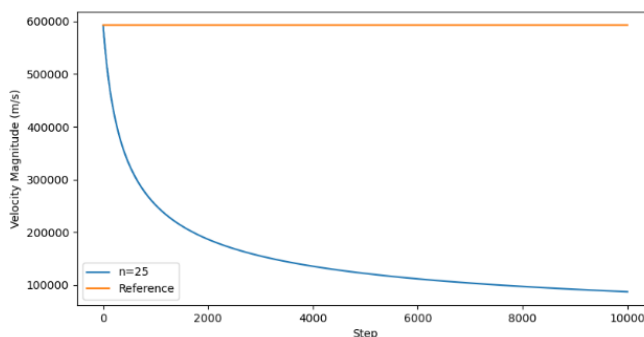


**Figure 13.** Comparison of velocity magnitude (m/s) vs. iteration step for  $n=25$  and reference

At later times, velocity decay almost converges, which is shown below.

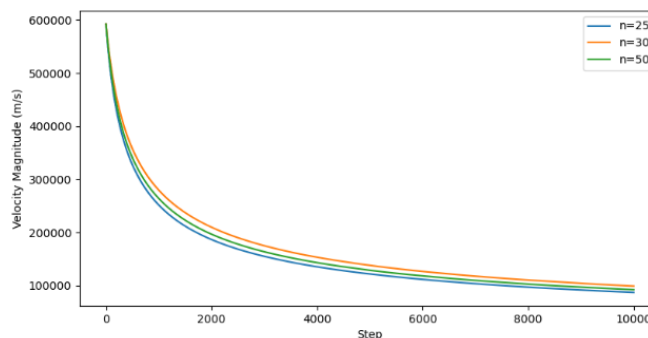


**Figure 14.** Velocity magnitude (m/s) vs. iteration step for several divisors for first 10000 steps

As shown in Figure 14, the decay of velocity magnitude for  $n = 50$  is a little bit larger compared to  $n = 30$ , which explains why the calculated error for  $n = 30$  is smaller than  $n = 50$ , as shown in Figure 10.

The result for case 2 is presented below.

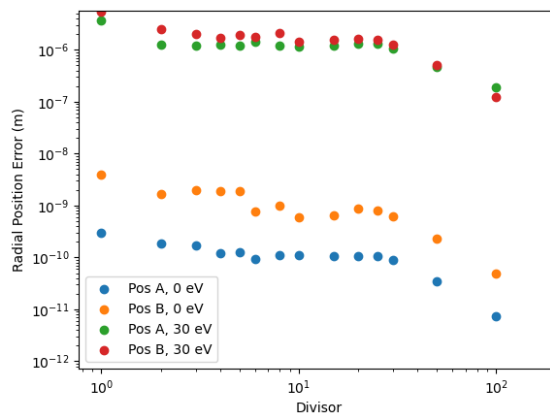


**Figure 15.** Radial position error (m) vs. divisor for various initial conditions

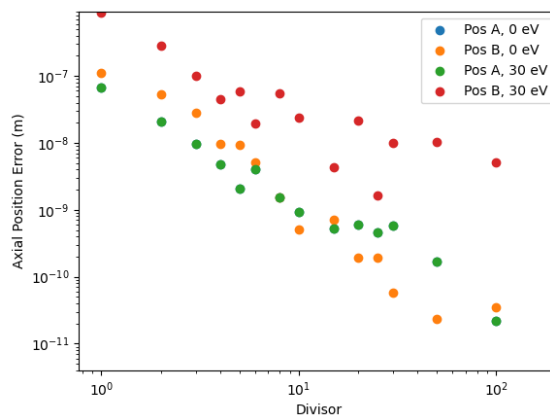


**Figure 16.** Axial position error (m) vs. divisor for various initial conditions

From Figures 15 and 16 above, the trend shows that the error decreases for enormous value of divisors. Some anomalies show up in Figure 16, which can be attributed to the somewhat erratic movement of the particle inside the ion chamber, i.e., too many unknown factors. For example, a slight alteration of particle trajectory might result in a different value of electric force felt by the particle, thus diverging the trajectory at later times. This is especially true when the electric field variation on spatial coordinate is significant, such as when a particle is placed with a relatively large initial radial position.

It is observed from figure 15 that for an initially stationary particle, a particle initially placed closer to the z-axis exhibits a minor radial position error. This is likely caused by electric field distribution, which has almost zero radial components near the z-axis. Thus, the particle only moves axially, reducing the error of the gyrating particle (which has a radial velocity component) close to the z-axis. It can be seen that when the initial position is further away from the z-axis, the error goes up.

The radial position error caused by the electric force is generally much smaller than when the particle is given initial radial velocity. If the particle is given a significant radial velocity component (which corresponds to 30 eV of kinetic energy), the error significantly increases, about a few thousand times higher.

The axial position error is relatively unaffected by initial radial velocity if the particle is placed close to the z-axis. This happened because the movement in the axial direction does not depend on the magnitude of radial velocity, assuming that the axial electric field is symmetric. For position A, the axial position error is identical (with a tiny error) between the static initial condition and the one with initial radial velocity. When the axial electric field varies with the radial position, the strength of axial force also varies with the radial position. Thus, the possible inaccuracies on radial position will cause the particle to have different axial electric force, increasing axial position error. Nevertheless, both radial position and axial position error are relatively small compared to the domain of simulation, which means that position-wise, time step width as high as 30 ps can be used in Penning simulation with this setup.

Figures 17 and 18 are the plots of particle trajectory on the z-r plane to grasp how a particle moves for various divisor values. Figures 17 and 18 show that the particle trajectory for  $dt = 3 \times 10^{-11}$  s (divisor = 1) looks jagged and does not match the reference trajectory of  $dt = 1 \times 10^{-15}$  s (divisor = 30000). For the initial radial position of  $r =$

0.1 mm, the trajectories of those two cases do not overlap with each other, while for  $r=3.5$  mm, although the trajectory for  $dt = 3 \times 10^{-11}$  s case still maintains its jagged form, the center of gyration almost coincides with the center of gyration of the reference. Although those figures suggest that the trajectory for  $dt = 3 \times 10^{-11}$  s case (and even for  $dt = 3 \times 10^{-12}$  s case) is not accurate, the magnitude of error is relatively small. For an initial radial position of 0.1 mm, the smallest radial position for all cases is about 0.08 mm, while the largest radial position is about 0.16 mm. Note that the domain of the simulation is  $r = [0, 5]$  mm and  $z = [0, 17.5]$  mm. Thus, the deviation is relatively small compared to the domain. The trajectory looks almost like a straight line compared to the simulation domain. Thus, it is shown that for small iterations,  $dt = 3 \times 10^{-11}$  s is effectively the same as  $dt = 1 \times 10^{-15}$  s, especially when many particles are involved.

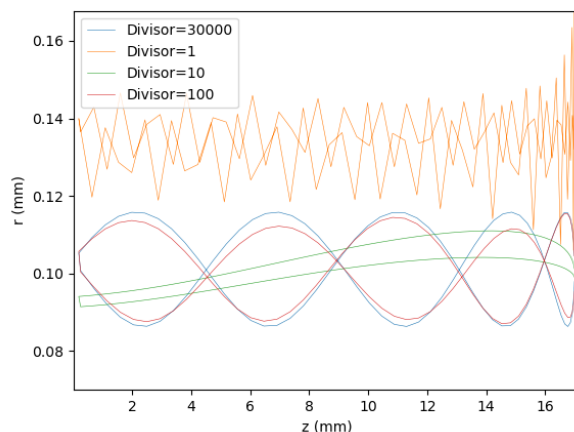


Figure 17. Trajectory plot for selected divisor, with the initial radial position of 0.1 mm and initial energy of 30 eV

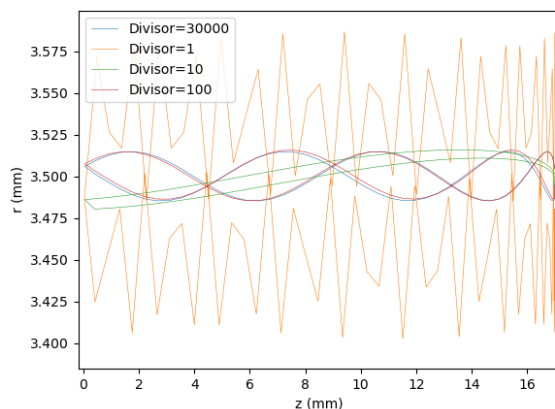
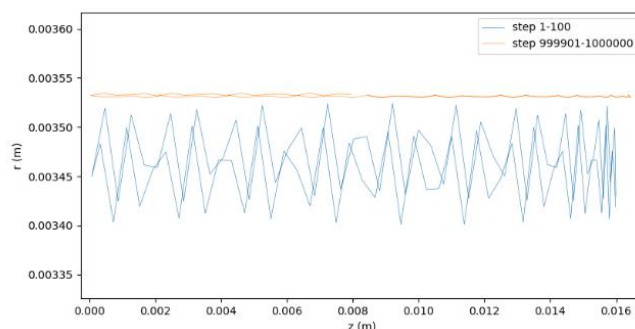


Figure 18. Trajectory plot for selected divisor, with the initial radial position of 3.5 mm and initial energy of 30 eV

It has been shown that the trajectory result compared to the big divisors is essentially identical for small iterations. It is essential to check whether it is the same for significant iterations since Abadi et al. [8] show that Penning simulation generally reaches its steady state after one million iterations (with  $dt = 30$  ps). Thus, the simulation here is extended to a million iterations. The plotted data is taken from steps 1 – 100 and 999901 – 1000000 to make analysis easier.



**Figure 19.** Trajectory plot for  $dt = 3 \times 10^{-11}$  s with the initial position of (16, 3.5) mm and initial energy of 30 eV

From Figure 19 above, it is apparent that non-axial velocity decreases with time. Thus at the latest steps, the particle almost entirely moves in a straight line. This confirms the finding from case 1, which shows that in the cylindrical Boris algorithm, the magnitude of the non-axial velocity (since  $v_z$  was not considered there) shrinks over time. A comparison with smaller time step width is needed to ensure that the pile-up of error causes this. The trajectory is shown below.

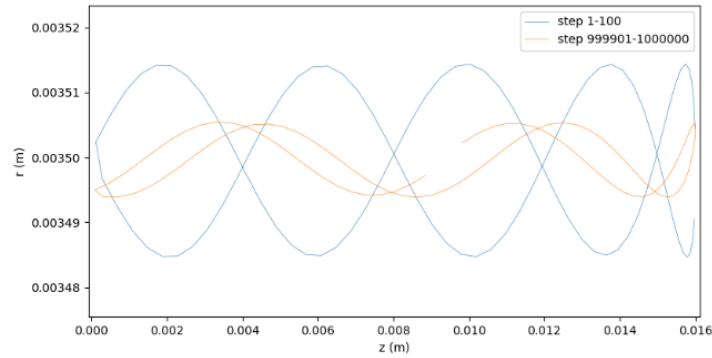


**Figure 20.** Trajectory plot for  $dt = 3 \times 10^{-13}$  s with the initial position of (16, 3.5) mm and initial energy of 30 eV

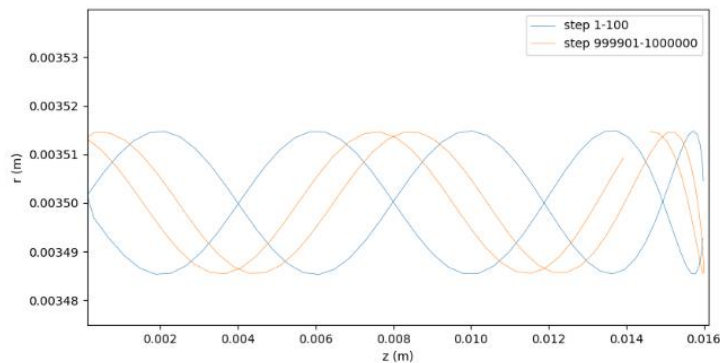


**Figure 21.** Trajectory plot for  $dt = 1 \times 10^{-15}$  s with the initial position of (16, 3.5) mm and initial energy of 30 eV

The results shown in Figure 20 and 21 confirms that the decrease in the magnitude of non-axial velocity is caused by the piling up of the error. Another case to consider is zero initial radial velocity since the error from Figure 19 shows that not only the magnitude of non-axial velocity was diminishing, but the center of gyration also changed. It will be easier to examine when the particle is stationary from the start.

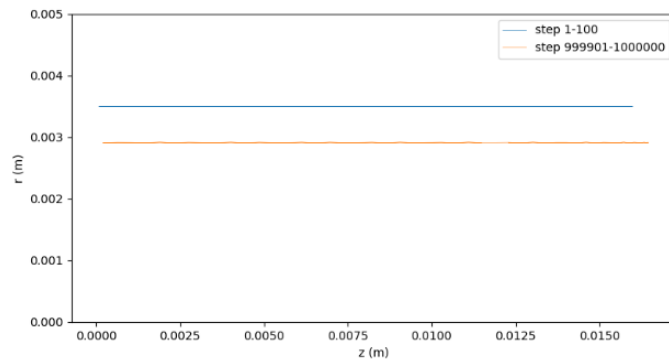


**Figure 22.** Trajectory plot for  $dt = 3 \times 10^{-11}$  s with the initial position of (16, 3.5) mm and initial energy of 0 eV

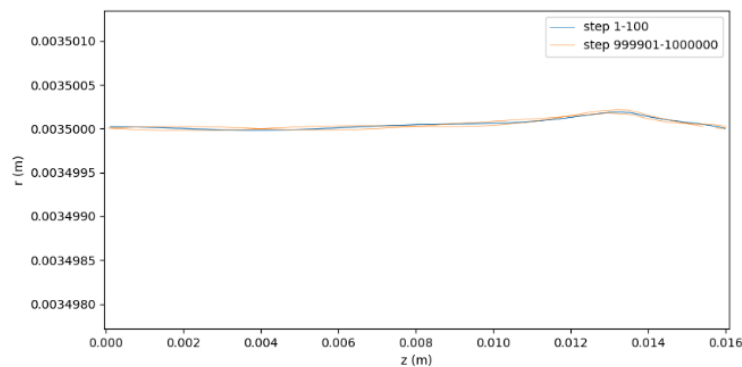


**Figure 23.** Trajectory plot for  $dt = 1 \times 10^{-15}$  s with the initial position of (16, 3.5) mm and initial energy of 0 eV

Figure 22 shows a significant change in radial position after many iterations. The average radial position does not change after many iterations for cases with much smaller time steps (thus the accuracy is much higher) as shown in Figure 23. There is also a subtle error in the axial direction. It can be noted that after an extensive iteration, the particle could reach points further than 16 mm (the particle's initial position). This is unphysical since energy conservation constrains the farthest axial position to be 16 mm.

Nevertheless, it can be seen that the discrepancy is relatively small (under 1 mm after a million iterations). Thus for the standard time step width, the axial error is acceptable. The results from Figure 17-19 indicate that the results for  $dt = 3 \times 10^{-11}$  s with typical parameters of Penning simulation are stable for various conditions, even though the error on non-axial velocity and on radial position might be significant.

The error of kinetic energy as a function of divisor for several values of initial conditions is plotted in Figure 24.

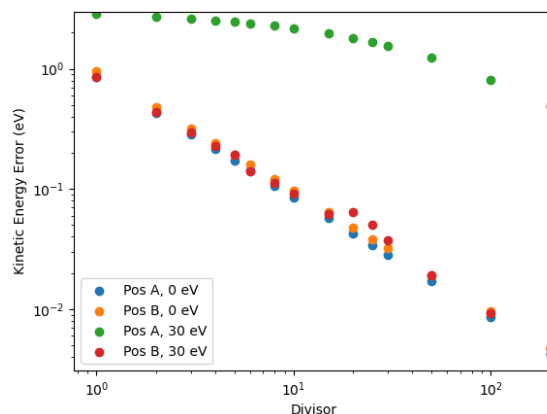


**Figure 24.** Kinetic energy error (eV) vs. divisor for various initial conditions

From Figure 24 above, it can be seen that, generally, the error follows a similar pattern. There is no significant difference in kinetic energy error for two different initial positions ( $r = 0.1$  mm and  $r = 3.5$  mm), as long as the initial kinetic energy equals zero. A similar result was also obtained when the initial kinetic energy was 30 eV with an initial position of  $r = 3.5$  mm, with a relatively small bump. The error increases significantly when the particle is initially situated at  $r = 0.1$  mm with an initial kinetic energy of 30 eV. The error also does not decrease as much as the error from other initial conditions when the divisor is increased. However, the magnitude of error of kinetic energy for the smallest divisor is around 2 eV, which is relatively small compared to the initial energy of 30 eV. This relatively small error might be important when collisional processes (such as ionization) are considered since some processes have a specific energy threshold to occur. For example, the ionization of hydrogen molecules and hydrogen atoms via



[15] has a threshold of 16 and 30 eV, respectively [15]. If the error causes the kinetic energy to be smaller than the threshold value, then the ionization might not happen (when it should be happening instead). Nevertheless, the simulation setup used here only considers a single charged particle moving in a vacuum, which means that the

presence of other charged particles inside the chamber does not hinder electric force from the cathode. This means that the acceleration directed to the z-axis might increase the kinetic energy up to 700 eV (related to cathode potential). Thus, a further investigation of the error of kinetic energy in a more proper simulation setup is necessary, which is not discussed in this paper.

Results presented above show that for Boris solver in cylindrical coordinates, even though the singularity problem can be avoided by passive rotation of the coordinate axis [10,11], the error near the z-axis is significant. This is especially important at the beginning of the simulation, where the particle is generated uniformly in space. A significant error might occur on particles close to the proximity of the z-axis.

The period of gyration of electrons for typically used magnetic field strength is usually on par with a good time step width used in Penning simulation. However, even though the time step width is larger than the gyration period of the particle and the trajectory of the particle at the typical time step width is way off the reference trajectory, "macroscopically," the results between large time step width and the reference are not that dissimilar (macroscopic in this context means when the simulation as a whole is considered, not just the trajectory of individual particles). The particle stays at a particular patch of the simulation domain and is generally stable for the simulation duration. The error does not cause the particle to stray off that far from the trajectory of the reference. One thing to watch out for is that for initially prominent radial positions, the mean radial position of the particle might substantially decrease for a large number of iterations, assuming that the particle stays at the domain for a long time (does not hit the wall or negatively ionize gasses inside the chamber). Results from case 1 and case 2 show that the particle tends to have a minor mean radial position than it should.

Overall, the result presented here shows that even though the exact trajectories of particles are distinctively different compared to reference data, the difference should not affect the simulation outcome much. For Penning simulation, a vast number of particles are simulated simultaneously. Thus, the "microscopic picture" and the exact values of trajectories are unimportant. Still, some errors build up over time, and if all simulated particles experience the same errors, then a macroscopic deviation might be observed. That being said, another solver which could constrain non-axial velocity decay might be a better option, as long as the additional computational cost is not much higher.

## CONCLUSION

It has been shown that the cylindrical Boris solver for typical values of parameters used in the Penning simulation is not accurate when the trajectory of particle per particle is observed. The mean of radial and axial positions does not differ much from the reference. Thus, when many particles are simulated simultaneously, the macroscopic result should be similar to the reference. The kinetic energy discrepancy between the typical time step width ( $dt=30$  ps) is also tiny compared to the time step width of the reference ( $dt = 0.001$  ps). However, the cylindrical Boris algorithm exhibits a unique error not found on cartesian Boris solver, which is the diminishing value of non-axial velocity as the simulation continues.

## ACKNOWLEDGMENTS

We express our gratitude to The Center for Accelerator Technology Research, especially Mr. Taufik and Mr. Silakhuudin, who have encouraged us with the making of this paper and for helpful discussion about the topic related to Penning ion source.

## REFERENCES

- [1] H. Qin, S. Zhang, J. Xiao, J. Liu, Y. Sun, and W. M. Tang, "Why is Boris algorithm so good?," *Phys. Plasmas*, vol. 20, no. 8, 2013, doi: 10.1063/1.4818428.
- [2] S. Zenitani and T. Umeda, "On the Boris solver in particle-in-cell simulation," *Phys. Plasmas*, vol. 25, no. 11, pp. 1–7, 2018, doi: 10.1063/1.5051077.
- [3] P. H. Stoltz, J. R. Cary, G. Penn, and J. Wurtele, "Efficiency of a Boris-like integration scheme with spatial stepping," *Phys. Rev. Spec. Top. - Accel. Beams*, vol. 5, no. 9, pp. 12–20, 2002, doi: 10.1103/PhysRevSTAB.5.094001.
- [4] X. S. Wei, Y. Xiao, A. Kuley, and Z. Lin, "Method to integrate full particle orbit in toroidal plasmas," *Phys. Plasmas*, vol. 22, no. 9, 2015, doi: 10.1063/1.4929799.
- [5] Silakhuudin and S. Santosa, "Conceptual design study of 13 MeV proton cyclotron," *Atom Indones.*, vol. 38, no. 1, pp. 7–14, 2012, doi: 10.17146/aij.2012.135.
- [6] I. G. B. Ed, "The Physics and Technology of Ion Sources," in *The Physics and Technology of Ion Sources*, <https://doi.org/10.55981/gnd.2023.6791>

2004. doi: 10.1002/3527603956.
- [7] J. L. Rovey, B. P. Ruzic, and T. J. Houlahan, "Simple Penning ion source for laboratory research and development applications," *Rev. Sci. Instrum.*, vol. 78, no. 10, pp. 1–4, 2007, doi: 10.1063/1.2791983.
- [8] M. Rafeian Najaf Abadi, M. Mahjour-Shafiei, and M. Yarmohammadi Satri, "Simulation and optimization of a negative hydrogen Penning ion source," *Phys. Plasmas*, vol. 25, no. 12, 2018, doi: 10.1063/1.5020224.
- [9] C. K. B. and A. B. Langdon, "Plasma Physics via Computer Simulation," McGraw-Hill, 1985.
- [10] G. L. Delzanno and E. Camporeale, "On particle movers in cylindrical geometry for Particle-In-Cell simulations," *J. Comput. Phys.*, vol. 253, pp. 259–277, 2013, doi: 10.1016/j.jcp.2013.07.007.
- [11] J. P. Boris, "Relativistic Plasma Simulation - Optimization of a Hybrid Code," Proc. 4th on Numerical Simulation of Plasmas, 1970.
- [12] B. Ripperda *et al.*, "A Comprehensive Comparison of Relativistic Particle Integrators," *Astrophys. J. Suppl. Ser.*, vol. 235, no. 1, p. 21, 2018, doi: 10.3847/1538-4365/aab114.
- [13] S. Zenitani and T. N. Kato, "Multiple Boris integrators for particle-in-cell simulation," *Comput. Phys. Commun.*, vol. 247, pp. 1–29, 2020, doi: 10.1016/j.cpc.2019.106954.
- [14] S.-V. B. Heidelberg, "Molecular Processes in Plasmas Collisions of Charged Particles with Molecules," 2007.
- [15] J. S. Yoon *et al.*, "Cross sections for electron collisions with hydrogen molecules," *J. Phys. Chem. Ref. Data*, vol. 37, no. 2, pp. 913–931, 2008, doi: 10.1063/1.2838023.
- [16] L. Brieda, "Plasma Simulation by Example 1st Edition," CRC Press, 2020.
- [17] T. Pang, "An Introduction to Computational Physics Second Edition," Cambridge University Press, 2006.
- [18] V. Vahedi and M. Surendra, "A Monte Carlo collision model for the particle-in-cell method: applications to argon and oxygen discharges," *Comput. Phys. Commun.*, vol. 87, no. 1–2, pp. 179–198, 1995, doi: 10.1016/0010-4655(94)00171-W.
- [19] J. P. Verboncoeur, "Particle simulation of plasmas: Review and advances," *Plasma Phys. Control. Fusion*, vol. 47, no. 5 A, 2005, doi: 10.1088/0741-3335/47/5A/017.
- [20] Silakhuddin and I. A. Kudus, "Study of development of the DECY-13 cyclotron based on applied physics learning," *J. Korean Phys. Soc.*, vol. 80, no. 9, pp. 880–886, 2022, doi: 10.1007/s40042-022-00434-w.